



Supplement of

**Impacts of irrigation on ozone and fine particulate matter (PM_{2.5})
air quality: implications for emission control strategies for intensively
irrigated regions in China**

Tiangang Yuan et al.

Correspondence to: Amos P. K. Tai (amostai@cuhk.edu.hk)

The copyright of individual parts of the supplement might differ from the article licence.

Table S1. Design of model experiments

Experiment	Irrigation	Anthropogenic emissions	Aerosol–radiation interaction & Aerosol–cloud interaction	Grid–nudging
CTL	Off	Normal	On	On
NOIRR	Off	Normal	Off	Off
IRR	On	Normal	Off	Off
Emiss_20c	On	NO _x and NH ₃ emissions are reduced by 20 %	Off	Off
Emiss_50c	On	NO _x and NH ₃ emissions are reduced by 50 %	Off	Off
Emiss_50NO _x	On	NO _x emissions are reduced by 50 %	Off	Off
Emiss_50NH ₃	On	NH ₃ emissions are reduced by 50 %	Off	Off

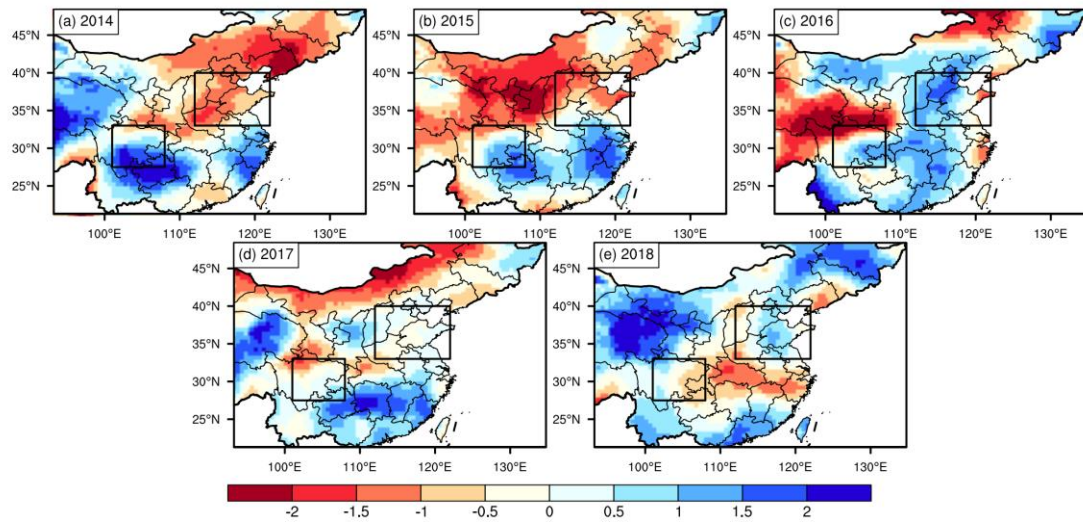


Figure S1. Spatial distribution of summertime Standardized Precipitation Evapotranspiration Index (SPEI) with 3-month timescale from 2014 to 2018.

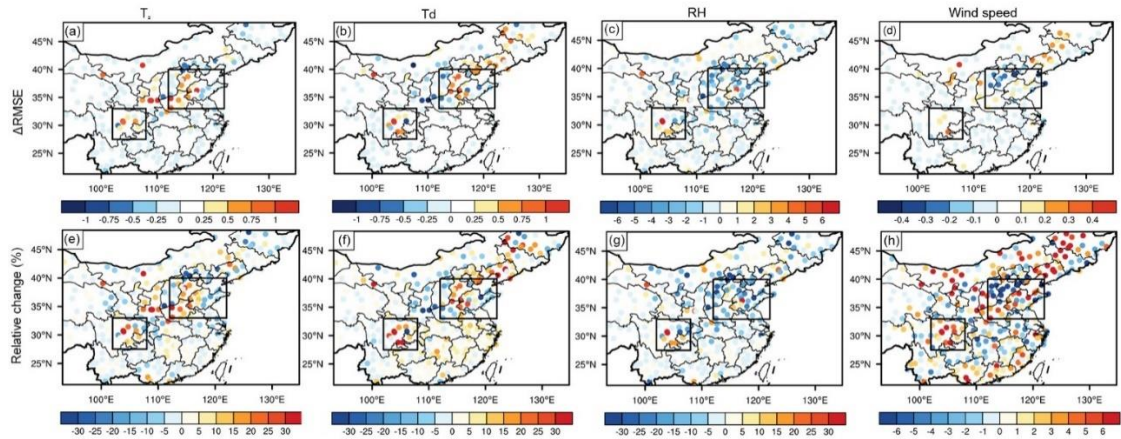


Figure S2. Changes in the root mean square error (Δ RMSE) of (a) air temperature at 2 m (T_2 , °C), (b) dew point temperature (T_d , °C), (c) relative humidity (RH, %) and (d) wind speed (m s^{-1}) against observations at each station over the model domain in IRR relative to NOIRR, and (e–h) the corresponding relative percentage changes (%). Positive values indicate reductions in RMSE due to irrigation, while negative values indicate increases in RMSE due to irrigation.

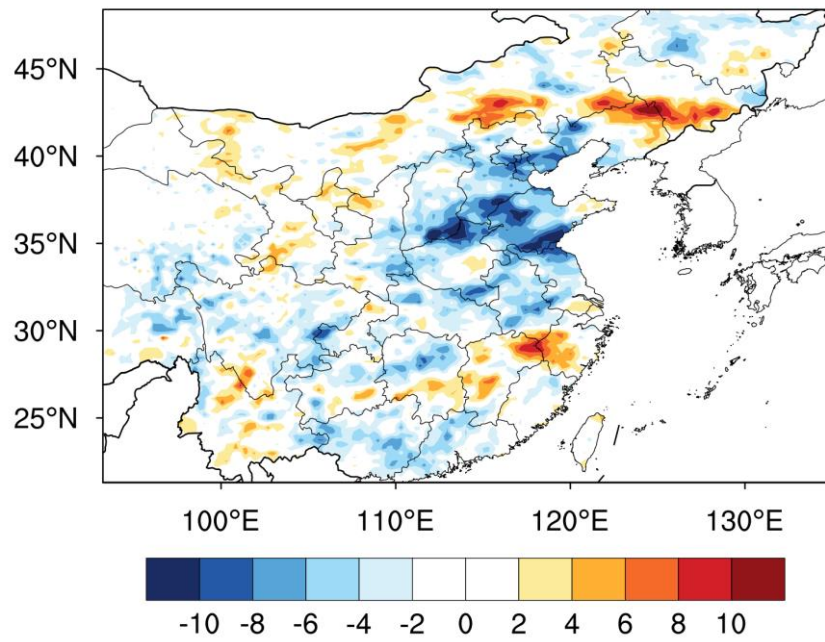


Figure S3. Spatial distribution of the change in downward solar radiation (W m^{-2}) in IRR relative to NOIRR averaged over the summer of 2017.

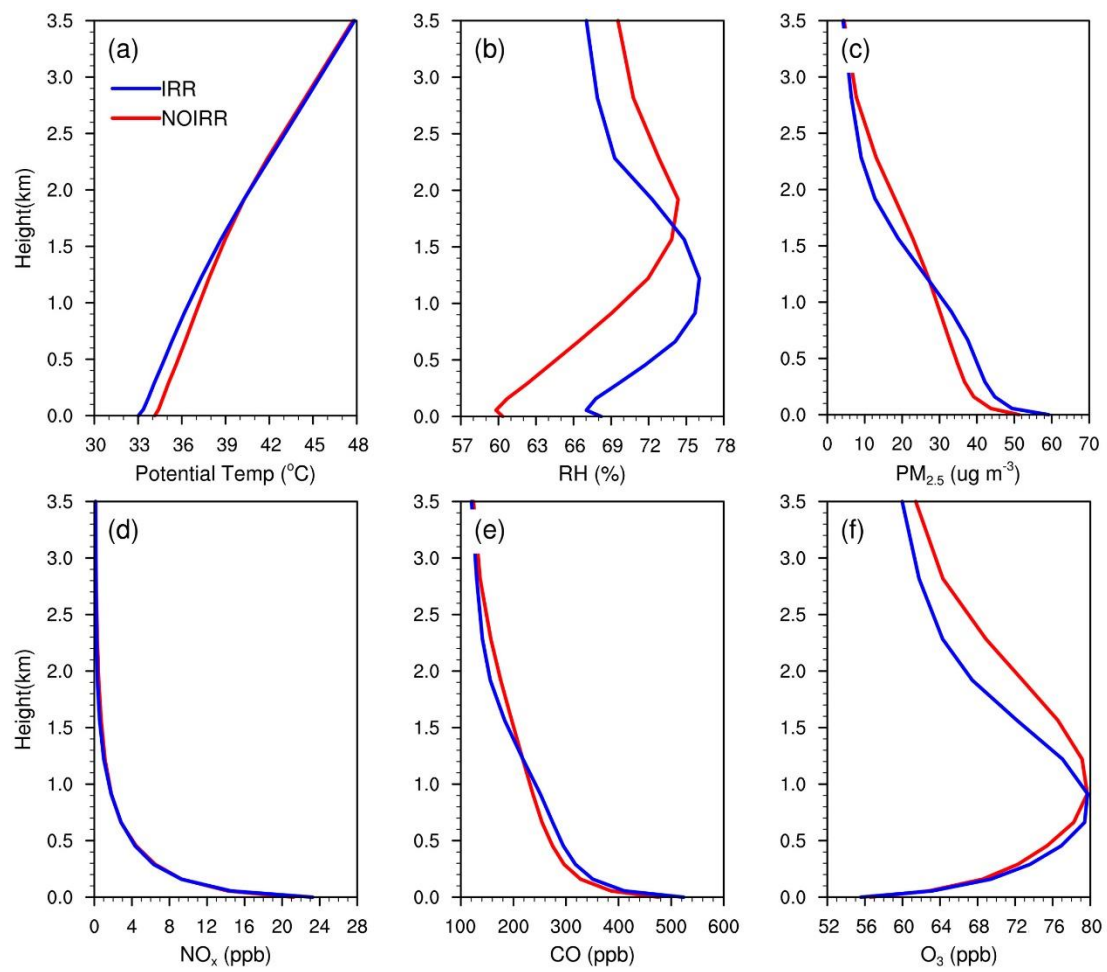


Figure S4. Vertical profiles of daily average potential temperature ($^{\circ}\text{C}$), RH (%), $\text{PM}_{2.5}$ ($\mu\text{g m}^{-3}$), NO_x (ppb), CO (ppb) and O_3 (ppb) from IRR (blue lines) and NOIRR (red lines) in Chengdu.

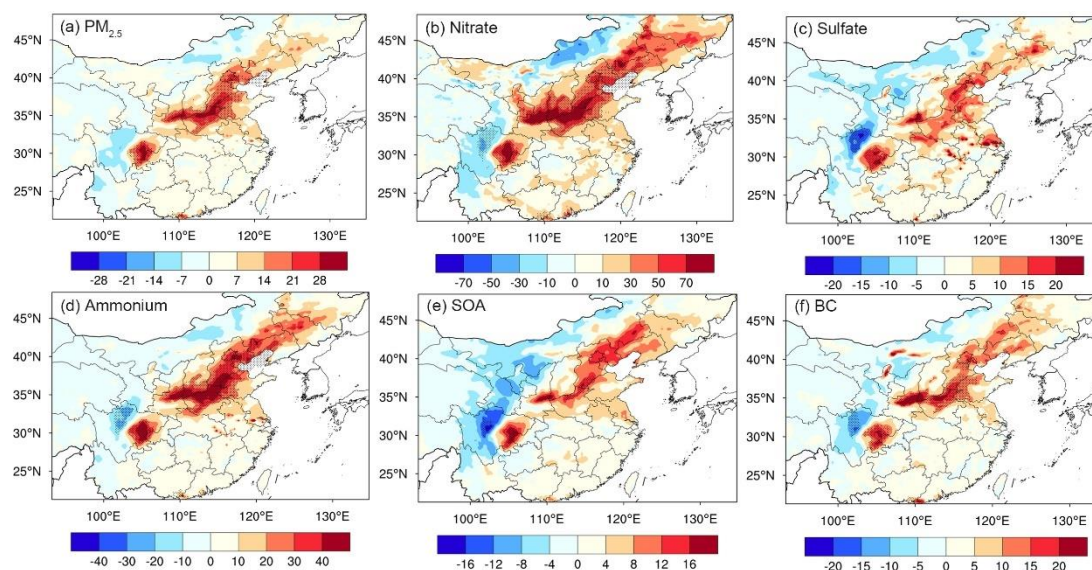


Figure S5. Spatial distribution of changes (%) in $PM_{2.5}$, nitrate, sulfate, ammonium, SOA and BC in IRR relative to NOIRR averaged over the summer of 2017. Dotted area indicates the changes are statistically significant at 95% confidence level using two-tailed Student's *t*-test.

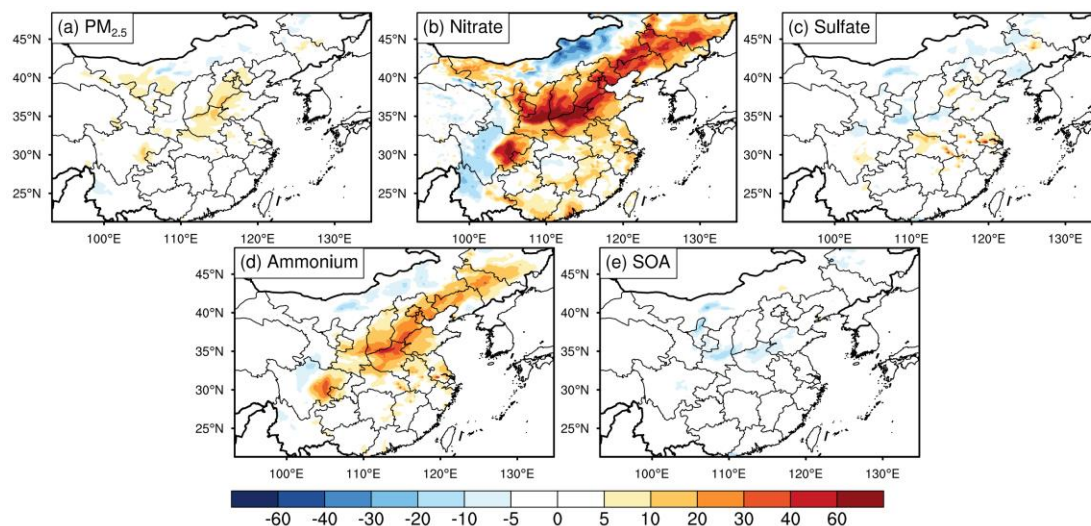


Figure S6. Contribution (%) of secondary formation to the increase in (a) $\text{PM}_{2.5}$ and (b–e) secondary components (nitrate, sulfate, ammonium and SOA). Contributions are calculated by subtracting the fractional changes in BC (ΔBC) from the fractional changes other secondary $\text{PM}_{2.5}$ components ($\Delta\text{PM}_{2.5}$), i.e., $\Delta\text{PM}_{2.5} - \Delta\text{BC}$.

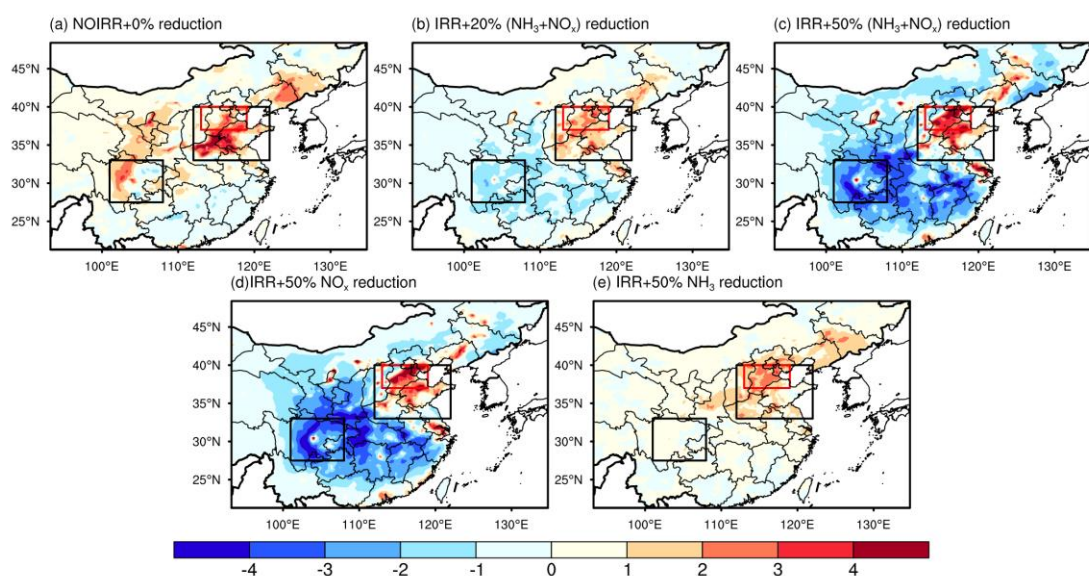


Figure S7. Spatial distribution of changes in nighttime ozone (ppb) in (a) NOIRR, IRR with (b) 20 % and (c) 50 % combined emission reduction of NO_x and NH₃, 50 % individual emission reduction of (d) NO_x and (e) NH₃, relative to IRR averaged over the summer of 2017. Black squares indicate North China Plain and Sichuan Basin, respectively. Red square is the city cluster of Beijing-Tianjin-Hebei region (BTH).